Simulation and Queueing Network Model Formulation of Mixed Automated and Non-automated Traffic in Urban Settings

by

Nathaniel Karl Bailey

B.S. Industrial Engineering and Operations Research
University of California Berkeley, 2010

SUBMITTED TO THE DEPARTMENT OF CIVIL AND ENVIRONMENTAL ENGINEERING IN PARTIAL FULFILLMENT OF THE REQUIREMENTS FOR THE DEGREE OF

MASTER OF SCIENCE IN TRANSPORTATION
AT THE
MASSACHUSETTS INSTITUTE OF TECHNOLOGY

SEPTEMBER 2016

Signature redacted

Signature of Author: _____
Department of Civil and Environmental Engineering
August 18, 2016

Signature redacted

Certified By: _____
Carolina Osorio Pizano
Assistant Professor of Civil and Environmental Engineering
Thesis Supervisor

Signature redacted

Accepted By: _____
Jesse Kroll
Professor of Civil and Environmental Engineering
Chair, Graduate Program Committee

Simulation and Queueing Network Model Formulation of Mixed Automated and Non-automated Traffic in Urban Settings

by

Nathaniel Karl Bailey

Submitted to the Department of Civil and Environmental Engineering on August 18, 2016 in Partial Fulfillment of the Requirements for the Degree of Master of Science in Transportation

ABSTRACT

Automated driving is an emerging technology in the automotive industry which will likely lead to significant changes in transportation systems. As automated driving technology is still in early stages of implementation in vehicles, it is important yet difficult to understand the nature of these changes. Previous research indicates that autonomous vehicles offer numerous benefits to highway traffic, but their impact on traffic in urban scenarios with mixed autonomous and non-autonomous traffic is less understood.

This research addresses this issue by using microscopic traffic simulation to develop understanding of how traffic dynamics change as autonomous vehicle penetration rate varies. Manually driven and autonomous vehicles are modeled in a simulation environment with different behavioral models obtained from the literature. Mixed traffic is simulated in a simple network featuring traffic flowing through an isolated signalized intersection. The green phase length, autonomous vehicle penetration rate, and demand rate are varied. We observe an increase in network capacity and a decrease in average delay as autonomous vehicle penetration rate is increased. Using the results of the simulation experiments, an existing analytical network queueing model is formulated to model mixed autonomous and non-autonomous urban traffic. Results from the analytical model are compared to those from simulation in the small network and the Lausanne city network, and they are found to be consistent.

Thesis Supervisor: Carolina Osorio Pizano
Title: Assistant Professor of Civil and Environmental Engineering

Acknowledgements

The research presented in this thesis was conducted with the assistance, support, and supervision of my co-advisor António Antunes at the University of Coimbra, as well as collaboration with Luís Vasconcelos at the Polytechnic Institute of Viseu.

The authors gratefully acknowledge support from the MIT Portugal Program (MPP) which provided funding via a grant for "Autonomous and cooperative urban mobility".

Contents

List of Illustrations

Table

Figures

Chapter 1

Introduction

As vehicles of increasing levels of automation and autonomy begin to make their way onto roadways, the need to understand what impacts they will have on transportation systems grows. While the development of new automated vehicle technologies has been rapid, research into their potential impacts in urban environments and the preparedness of cities and transportation planners has lagged behind. Several companies such as Google [1] and Uber [2] have tested autonomous vehicles on public roadways, with Google self-driving cars having logged over 1.8 million miles [1]. Tesla made public in 2015 an Autopilot feature which allows their Model S vehicles to control acceleration, braking, steering, and lane changing [3]. In contrast, only 6% of major US cities' transportation plans considered the effects of driverless technologies in 2015 [4].

Automated driving can refer to a wide range of self-driving capabilities. The National Highway Traffic Safety Administration (NHTSA) has developed a classification system that allows for specificity when referring to automated vehicles [5]. This classification system begins at Level 1, at which some individual vehicle controls, such as stability control or braking, are automated. It ends at Level 4, at which point the vehicle is able to manage all safety-critical functions entirely on its own without requiring a human driver at all. Although Level 4 automated vehicles remain somewhat futuristic at this point, vehicles at Levels 2 and 3, in which the driver is able to rely solely on the vehicle for a large portion of safety-critical functions, are readily being tested at the present. Although these vehicles are not truly autonomous as they do not act independently, we will refer to vehicles at Level 2 and higher as autonomous vehicles for the rest of the paper, as this is the term that has entered the common lexicon.

When these autonomous vehicles become widely available to the public, they are likely to drive much differently than humans do. One of the major promises of automated driving is the potential to improve safety by sharply reducing collision rates. Of the 6.1 million reported vehicle collisions in 2014, over 90% are attributed to driver error [6]. Other features of autonomous vehicles may include reduced reaction times and control strategies which lead

to more stable traffic and other benefits [7]. In the near term, autonomous vehicles will likely share the roadways with human drivers, requiring consideration of the traffic patterns resulting from mixed autonomous and non-autonomous traffic. Differences in driving patterns and the interactions between autonomous and human-driven vehicles will mean that traffic featuring autonomous vehicles will behave differently than traffic existing today, potentially triggering changes in traffic management strategies.

Microscopic traffic simulation is a valuable tool to develop understanding of the behavior of this mixed traffic and how this behavior changes as the proportion of autonomous vehicles increases, thus accounting for a wide range of possible scenarios for the adoption of autonomous vehicles. Although much attention has been paid to traffic simulation experiments in highway scenarios, research detailing these patterns is lacking in the urban context. As cities prepare to make infrastructure investments for their future, they are put at risk by lacking this knowledge. It is thus imperative to understand the impacts that autonomous vehicles have on urban traffic for the purpose of developing improved traffic management strategies.

In this thesis, we outline the results of simulation experiments which inform our understanding of how traffic dynamics change as autonomous vehicle penetration increases within a network. These insights are used to formulate an analytical queueing network model which can be used to estimate the average travel time of traffic within an urban network featuring a mixture of autonomous and non-autonomous traffic. In the future, this analytical model can be incorporated into a simulation-based optimization framework to inform transportation planners and researchers on the impacts that different traffic management strategies will have as autonomous vehicles are introduced into urban environments.

In chapter 2, we examine existing literature on the simulation of autonomous vehicles, and observed traffic impacts in urban and freeway scenarios. We then present in chapter 3 an overview of the implementation of autonomous vehicles in our simulation experiments. The results of experiments which simulate a mixture of autonomous and manually driven vehicles in urban traffic environments are presented. We simulate flow through a signalized intersection on a one-lane road under various signal timing schemes and observe the impact of autonomous vehicle penetration rate and traffic flow on throughput and travel time. In chapter 4, the results of the simulation experiments are used to formulate an analytical model which estimates average travel time by representing the road network as a series of queues. This queueing model is evaluated via comparison to simulation results to judge its applicability. This comparison is performed both for the simple network described in

Chapter 3, as well as for a large-scale city network in Lausanne, Switzerland. Finally, in Chapter 5, we discuss the results of this work and outline future steps we plan to take in using the formulation and the analytical model to solve traffic optimization problems.

This thesis is a continuation of previous research by Bailey, Osorio, Antunes, and Vasconcelos presented at the Mobil.TUM 2015 International Scientific Conference on Mobility and Transport in an article entitled "Designing traffic management strategies for mixed urban traffic environments with both autonomous and non-autonomous vehicles" [8]. That article presents a literature review of existing work in this field, as well as the design and results of the simulation experiments presented in Chapter 3 of this thesis. This thesis updates and elaborates upon the literature review and simulation work presented in that paper in Chapters 2 and 3 respectively, as well as presenting novel work in the formulation of an analytical network queueing model in Chapter 4.

Chapter 2

Existing Work

2.1 Behavioral Models of Autonomous Vehicles

In order to accurately simulate autonomous vehicles, we must first develop ways to model the driving behavior they exhibit. The driving behavior of vehicles in microscopic traffic simulation is governed by several functions, including car following, lane changing, and gap acceptance. Car following behavioral models govern the longitudinal speed and acceleration of a vehicle, controlling the gap between a vehicle and the vehicle directly ahead of it. Lane changing and gap acceptance models control the vehicle's lane changing logic, determining when it is acceptable to change lanes and how to do so.

Car following in autonomous and semi-autonomous vehicles is currently the subject of much development and research. Adaptive cruise control (ACC) systems are currently being implemented in vehicles by manufacturers and researchers [9, 10] as an automated driver assistance tool to allow drivers to relinquish longitudinal control of their vehicle and focus only on steering. While fully autonomous vehicles may also control the steering, the longitudinal control may be modeled similarly.

ACC systems use radar and other sensing technologies to determine the leading vehicle's distance and speed, and translate this information into acceleration and braking commands which are delivered to the vehicle by a controller. Ntousakis et al. [11] provide a thorough review of existing ACC models and recent developments in the field.

Cooperative adaptive cruise control (CACC) is a further extension of ACC that supplements information gathered by the vehicle's own sensors with telecommunication systems that allow connected vehicles to exchange information wirelessly. This provides a vehicle equipped with CACC with more information about the vehicle it is following, provided that vehicle is also equipped with compatible telecommunication systems. It also is able to communicate and engage in complex maneuvers, such as forming platoons with other CACC vehicles [12]. Alternatively, CACC vehicles may connect to and receive information from

infrastructure, resulting in vehicle-to-infrastructure (V2I) systems rather than vehicle-to-vehicle (V2V).

2.2 Microscopic Traffic Simulation

Of particular interest is the impact that vehicles equipped with different ACC and CACC systems have on traffic characteristics. Understanding the characteristics of traffic which contains a mix of autonomous and manually driven vehicles. The literature regarding these impacts seems to contain three main categories of simulated scenarios: single lane highways, multiple lane highways, and ring roads.

Many researchers have simulated ACC and CACC vehicles on single lane highways to observe how an increase in the penetration rate of these semi-autonomous vehicles affects traffic dynamics. Simulations which use variations of the Intelligent Driver Model (IDM) proposed by Treiber et al. [13] have found that if 30% of traffic is made up of ACC vehicles, delays created by rush hour traffic at an on-ramp can be eliminated [14]. With ACC vehicles using a car-following model proposed by Wang and Rajamani [15], Ntousakis et al. found that with desired time gaps less than 1.1 seconds, highway capacity increased linearly with the penetration rate of ACC vehicles [11]. However, for desired time gaps of 1.5 seconds or more, capacity decreased as ACC penetration rate increased.

Shladover et al. [10] simulated a one-lane highway with a mix of ACC vehicles, CACC vehicles with V2V communication, and manually driven vehicles. Time gap settings for ACC and CACC vehicles were chosen to match the settings chosen by human passengers in previous field tests [16]. 31% of the ACC vehicles used a 2.2 second time gap, 18.5% used a 1.6 second time gap, and 50.4% used a 1.1 second time gap. For CACC vehicles, the time gaps were much lower: 12% used a 1.1 second time gap, 7% used a 0.9 second time gap, and 57% used a 0.6 second time gap. Simulations demonstrated that with these settings, increased penetration rate of CACC equipped vehicles had significant impacts on traffic flow. For CACC penetration rates above 50%, a statistically significant increase in lane capacity was observed. When all vehicles were equipped with CACC, the lane capacity approximately doubled from the baseline 2,000 vehicles per hour to roughly 4,000. The penetration rate of ACC vehicles, however, had little effect on traffic flow.

Multi-lane highway simulations are more complicated due to the interactions created by lane changing. Using an enhanced IDM with a constant-acceleration heuristic used in

non-critical situations, simulations of a multiple-lane highway demonstrated that vehicles using this car following model could improve traffic flow and recovery from traffic breakdowns.Maximum traffic flow was increased by 0.3% and the outflow from traffic jams was increased 0.24% per 1% increase in the proportion of ACC vehicles on the roadway [9].

Arnaout and Arnaout [17] simulated a multi-lane highway with a mix of CACC vehicles and manually driven ones. At low levels of vehicle flow reflecting moderate traffic, there was found to be no statistically significant difference between cases with varying amounts of CACC vehicles. In heavy traffic conditions, however, an increase in CACC vehicles was found to lead to a significant increase in traffic flow. However, for CACC penetration rates of less than 40%, the effect was minimal. Van Arem et al. similarly found that low penetrations of CACC below 40% had little effect on traffic characteristics, but found that higher penetration rates were able to improve traffic stability and throughput in the presence of a lane drop from five to four lanes [18].

Simulations on enclosed ring roads are designed to observe the creation of traffic jams due to the effects of car-following and variations in speed. Jerath and Brennan [19] modeled ACC systems by using the GM fourth model [20], which parameterizes drivers' sensitivities to external stimuli with a parameter α, where higher values of α correspond to faster reaction times. The authors modeled human drivers with $\alpha = 0.4$ and ACC-equipped vehicles with $\alpha = 0.7$, and experiments showed that the critical density at which traffic jams form increases as ACC penetration increases, although it also becomes more sensitive to an increase in human-driven vehicles. Ntousakis et al. found that higher penetration of ACC vehicles led to more stable traffic on ring roads by reducing the intensity and quantity of congestion waves [11].

Based on the literature regarding microscopic traffic simulation of ACC and CACC vehicles, it seems that the introduction of autonomous and semi-autonomous vehicles has positive impacts on highway traffic flow and lane capacity. Across many different studies making different assumptions about car-following behavior, lane changing behavior, and connectedness, there is a common trend showing that increased penetration of autonomous vehicles leads to increased capacity and flow. However, the question of how autonomous vehicles may impact traffic in urban conditions is still an open question, as the majority of the literature we are aware of has focused on simulations of highway conditions.

In contrast to the abundance of car following models, lane changing and gap acceptance models for the simulation of autonomous vehicles are not as developed. The tactical decisions

required for lane changing are complex to model and computationally intensive to solve, especially compared to the operational level decisions required for car following [21]. Many intelligent systems have been developed to control lane changing decisions, including the use of neural networks [22], dynamic probabilistic networks [23], and game theoretic approaches [24], though few of these approaches have been applied to microscopic traffic simulation.

Although agent-based models of the driving behavior of autonomous vehicles are common, large-scale analytical models that represent mixed autonomous traffic in large transportation systems are more scarce. Research by Bose and Ioannou focuses on analytical descriptions of highway traffic which includes semi-automated vehicles [25]. This research formulates the flow-density diagram of a highway with 100% semi-automated vehicle traffic in an analytical manner, and also models stop-and-go traffic in a mixed traffic scenario with an M/M/1 queue to determine the average delay experienced. They find that the presence of semi-automated vehicles results in greater traffic flow rate for the same traffic density, and reduces the average delay experienced by vehicles.

Levin and Boyles [26] developed a formulation for a multiclass cell transmission model with mixed autonomous and human traffic based on a collision avoidant car following model, and analysis indicated that as autonomous vehicles penetration rate increases, the capacity of a roadway increases. The findings from these analytical formulations are similar to the simulation results discussed above.

Overall, the literature regarding mixed traffic featuring both autonomous and human-driven vehicles provides a thorough examination of the simulation of this traffic in highway scenarios. Through the use of a variety of ACC and CACC models representing the behavior of autonomous vehicles, these experiments mostly indicate that increasing penetration of autonomous vehicles on highways results in positive impacts on traffic patterns. Additionally, some research into analytical models of mixed highway traffic points towards the same conclusions. However, the literature does not provide many examples of simulations which incorporate different lane-changing or other driving behaviors into autonomous vehicles. It also fails to cover the topic of how mixed autonomous and non-autonomous traffic in urban environments behaves.

Chapter 3

Simulation Experiments

3.1 Introduction

Microscopic traffic simulation is a valuable tool to gain an understanding of the behavior of mixed traffic involving both autonomous and non-autonomous vehicles. In this chapter, we detail the results of experiments using microscopic traffic simulation, conducted with the simulation software Aimsun (version 8.0) [27], to model the impact that the addition of autonomous vehicles has on urban traffic. These experiments focus on traffic flowing through a signalized intersection, an important feature in understanding the behavior of traffic in urban environment. An understanding of how autonomous vehicles impact the traffic dynamics of signalized intersections will provide insight into their impact on urban traffic as a whole.

These simulation experiments model a small network with traffic consisting of a mix of autonomous vehicles and manually driven ones. The two types of vehicles obey differing behavioral models which reflect the differences in driving between autonomous vehicles and manually driven ones. This chapter first details the behavioral models used in these simulations. Next, an overview of the simulation experiments is provided, and the results are presented and discussed.

3.2 Behavioral Models

In order to use microscopic traffic simulation to develop an understanding of mixed autonomous and non-autonomous urban traffic, each class of vehicle must be designated behavioral models to govern their driving behavior in the simulator. These models should be as representative of reality as possible, both for autonomous and manual vehicles, so as to yield accurate understanding of traffic dynamics and to benefit future work which aims to inform the decisions of actual urban traffic management.

Behavioral models for human-driven vehicles are well-researched and can be compared to a wealth of data taken from the field to investigate accuracy [28, 29]. By contrast, analytical behavioral models for autonomous vehicles are more speculative, and it is difficult to assess their accuracy as there is limited data from field tests of autonomous vehicles in urban traffic. Because of this, the behavioral models used for autonomous vehicle in this research are selected from those present in the literature based on assumptions and reasoning made by the author which will be explained in detail below. In the future, more detailed, field-tested models may become available, which can be used within this framework to gain a better understanding of urban traffic management with autonomous vehicles.

3.2.1 Manually Driven Vehicles

In these simulation experiments, manually driven vehicles were represented by vehicles which use the default car-following model implemented in Aimsun [30], which is based on the Gipps model [31] and accounts for local variables such as the speed limit of the roadway, the vehicle's acceptance of the speed limit, and the speed of cars in adjacent lanes. This car-following model has been demonstrated to accurately reflect driving behavior gathered in field studies when compared to other commonly used models in microscopic traffic simulators [28, 29].

The Gipps model dictates that the maximum speed of vehicle i during the time interval $(t, t+T)$ is the minimum of the following two equations:

$$V_a(i, t+T) = V(i,t) + 2.5a(i)T\sqrt{1 - \frac{V(i,t)}{V^*(i)}\left(0.025 + \frac{V(i,t)}{V^*(i)}\right)} \tag{3.1}$$

$$V_b(i, t+T) = d(i)T + \sqrt{d(i)^2T^2 - d(i)\left[2\left[x(i-1,t) - s(i-1) - x(i,t)\right] - V(i,t)T - \frac{V(i-1,t)^2}{d'(i-1)}\right]} \tag{3.2}$$

Equation 3.1 defines V_a, the vehicle's velocity during the following time step during the following time step if there are no obstacles preventing its acceleration. $V(i,t)$ is the speed of vehicle i at time t, $V^*(i)$ is vehicle i's desired speed, which depends on the driver's preference and the speed limit of the road section, $a(i)$ is vehicle i's maximum possible deceleration,

and T is the reaction time in seconds. The acceleration in a time step decreases as the vehicle approaches its desired speed.

Equation 3.2 defines V_b, the upper bound of speed that the vehicle is able to travel while safely avoiding a crash if the leading vehicle begins to decelerate. $d(i)$ is the maximum deceleration desired by vehicle i ($d(i) < 0$), $x(i,t)$ is the position of vehicle i at time t, $x(i-1,t)$ is the position of the leading vehicle $(i-1)$, $s(i-1)$ is the leading vehicle's length, and $d'(i-1)$ is the vehicle's estimation of the leading vehicle's desired deceleration. The actual velocity that the vehicle takes at the next time step is the minimum of V_a and V_b.

3.2.2 Autonomous Vehicles

As discussed previously, the choice of behavioral models to represent automated driving in the simulation environment requires many assumptions because of the uncertainty of how autonomous vehicles will behave when introduced in urban environments in the real world. This research focuses on vehicles with Level 2 or 3 of automation using NHTSA's classification [5], where the driver can fully cede control of acceleration and braking to the vehicle, but will need to control the vehicle to change lanes and perform other tasks. This is largely because of a scarcity of models for autonomous lane changing in microscopic traffic simulation, meaning that we have no basis to predict how autonomous vehicles may behave differently than manually-driven ones in this regard. The autopilot feature in the Tesla Model S, one of the most sophisticated automated driving features widely available today, operates somewhere between Levels 2 and 3 in the NHTSA classification system [32] but is not designed for use in urban areas [3]. Thus, these assumptions about urban automated driving seem reasonable for vehicles deployed in the near future.

Additionally, we make the assumption that these semi-automated vehicles feature no connectivity or communication with other vehicles or infrastructure. Assuming no connectivity reduces the number of assumptions which we make regarding the nature of automated driving. Connected vehicles may be capable of complex maneuvers such as platooning [12] and enhanced merging [18] which make it difficult to predict exactly how connected autonomous vehicles may behave once implemented in roadways. Because the exact mechanics of connected autonomous driving are still the subject of research and debate, limiting this research to the scope of unconnected vehicles allows it to reflect more accurately the near-term impacts of automated driving in urban environments.

To represent the acceleration and braking behavior of autonomous vehicles in this research, we use the Enhanced Intelligent Driver Model (EIDM) proposed by Kesting et al. [9] which combines the Intelligent Driver Model (IDM), originally used to represent human driving, with a constant-acceleration heuristic to use in non-critical braking situations. This can occur, for example, when a car changes lanes in front of the vehicle, causing the gap to be less than desired.

The IDM dictates the acceleration of the vehicle using the following equations:

$$a_{\text{IDM}}(s, v, \Delta v) = a\left[1 - \left(\frac{v}{v_0}\right)^{\delta} - \left(\frac{s^*(v, \Delta v)}{s}\right)^2\right] \tag{3.3}$$

$$s^*(v, \Delta v) = s_0 + vT + \frac{v\Delta v}{2\sqrt{ab}} \tag{3.4}$$

This equation calculates the acceleration of an EIDM-equipped vehicle given values of the gap distance s, the velocity of the EIDM vehicle v, and the difference in velocities between it and the leading vehicle, Δv. The parameters are as follows: v_0 is the desired speed of the IDM vehicle, T is the desired time gap, s_0 is the jam distance, a is the maximum acceleration, b is the desired deceleration, and δ is the free acceleration exponent.

Equation 3.4 finds the desired safe gap distance $s^*(v, \Delta v)$ between the EIDM vehicle and the leading vehicle. Equation 3.3 then combines an acceleration strategy for an open road with a braking strategy if the actual gap distance is smaller than this desired safe gap. In addition to this, the EIDM incorporates a constant-acceleration heuristic (CAH) which changes the braking strategy in non-critical situations where the IDM may have a tendency to overreact to actual gap distances which are shorter than desired. This heuristic is used as an indicator which informs the EIDM-equipped vehicle whether a braking situation is critical or not, and adjusts the IDM acceleration accordingly.

The CAH uses as inputs the gap distance s, the EIDM vehicle's speed v, the leading vehicle's speed v_1, and the leading vehicle's acceleration a_1. The accelerations given by the CAH and EIDM are given in the following equations, where c is a "coolness factor" which determines the weights placed on the CAH and IDM, $\Theta(x)$ is the Heaviside step function, and $\tilde{a}_l$ is the maximum of a and a_1, the accelerations of the ego vehicle and the leading vehicle, respectively:

$$a_{\mathrm{CAH}}(s, v, v_1, a_1) = \begin{cases} \frac{v^2 \tilde{a}_l}{{v_1}^2 - 2s\tilde{a}_l} & \text{if } v_1 (v - v_1) \leq -2s\tilde{a}_l \\ \tilde{a}_l - \frac{(v-v_1)^2 \Theta(v-v_1)}{2s} & \text{otherwise} \end{cases} \tag{3.5}$$

$$a_{\mathrm{EIDM}} = \begin{cases} a_{\mathrm{IDM}} & \text{if } a_{\mathrm{IDM}} \geq a_{\mathrm{CAH}} \\ (1-c)\, a_{\mathrm{IDM}} + c \left[a_{\mathrm{CAH}} + b \tanh\left(\frac{a_{\mathrm{IDM}} - a_{\mathrm{CAH}}}{b} \right) \right] & \text{otherwise} \end{cases} \tag{3.6}$$

Equation 3.5 gives the CAH acceleration, which is the maximum acceleration which leads to no collisions under the assumptions that the leading vehicle's acceleration does not change over the near future and that drivers are able to react without delay. The acceleration given by the EIDM is provided in Equation 3.6. It first determines whether the IDM or the CAH gives a higher value for acceleration under the current conditions. If the IDM acceleration is greater than or equal to the CAH acceleration, the EIDM vehicles uses the IDM acceleration as it is assured of being crash-free under all circumstances. If the IDM acceleration is less than the CAH acceleration, but the CAH acceleration is comfortable (greater than $-b$, the maximum desired deceleration), the vehicle undergoes mild braking assuming a mildly critical situation. If both the IDM and CAH accelerations are extreme (less than $-b$), the vehicle is in a critical situation and cannot exceed either acceleration provided.

The EIDM was designed for use in semi-autonomous vehicles and has already been implemented in test vehicles [9], making it an appropriate model to use when simulating automated urban driving. Vehicles equipped with the EIDM have been shown to result in increased lane capacity with increased penetration rates during simulations run on multi-lane highways. Additionally, it has proven to hold string stability, and to behave well at all velocity ranges [9]. This is critical for ACC systems which are used in urban environments, such as in these experiments, where speeds may vary widely.

The semi-automated vehicles in the simulation also differ from manual vehicles in some parameters of the microscopic simulator. When a parameter exists in both the Gipps car following model and the EIDM, we choose to use the mean value for manually driven vehicles, obtained via calibration [30], as the value for all autonomous vehicles. The autonomous vehicles have no variation in these parameters, which means that each individual vehicle behaves the same. For parameters unique to the EIDM, we use the values suggested in the original paper [9]. Additionally, Aimsun introduces several reaction time parameters, for which we use the default values for non-autonomous vehicles, and a value of 0.1 seconds for

Parameter	Mean (HV)	Deviation (HV)	Min (HV)	Max (HV)	Value (AV)
Desired Speed (km/hr)	110	10	80	150	110
Speed Acceptance	1.1	0.1	0.9	1.3	1.1
Minimum Gap (m)	1	0.3	0.5	1.5	1
Reaction Time (s)	0.8	0	0.8	0.8	0.1
Reaction Time at Stop (s)	1.2	0	1.2	1.2	0.1
Reaction Time at Traffic Signal (s)	1.6	0	1.6	1.6	0.1
Max Acceleration (m/s^2)	3	0.1	2.6	3.4	3
Max Deceleration (m/s^2)	6	0.5	5	7	6

Table 3.1: The values used for parameters common to human-driven vehicles (HV) and semi-autonomous vehicles (AV) in simulation. Parameters for non-autonomous vehicles have a standard deviation, minimum, and maximum, while the parameters are identical across autonomous vehicles.

the semi-autonomous vehicles. Table 3.1 details the values of the parameters used for each type of vehicle.

To demonstrate the differences between the two types of vehicles, an analytical experiment is shown in Figure 3.1 comparing the response of following vehicles of each class to a leader vehicle which undergoes a series of accelerations and decelerations. The leader, which starts 50 meters ahead of the following vehicle, has its speed profile plotted in the solid line. The speed of a following autonomous vehicle using the EIDM car-following model with parameters as described above is plotted in the dotted line. The speed of a following manually driven vehicle using the Gipps car-following model with parameters taking the mean of the distribution described above is plotted in the dashed line.

Looking at this figure gives a sense of how the two classes of vehicle react to different circumstances. The EIDM vehicle reacts more quickly to urgent situations, such as the sharp braking near 60 seconds. It both initiates deceleration sooner than the Gipps vehicle and slows down to match the leader's speed more quickly. It also features smoother accelerations when compared to the sharp changes in speed that the Gipps vehicle experiences, for example around 15 seconds.

3.3 Experimental Design

Using these behavioral models for the different classes of vehicles simulated, simulation experiments were developed with the aim of understanding the effects that increased autonomous

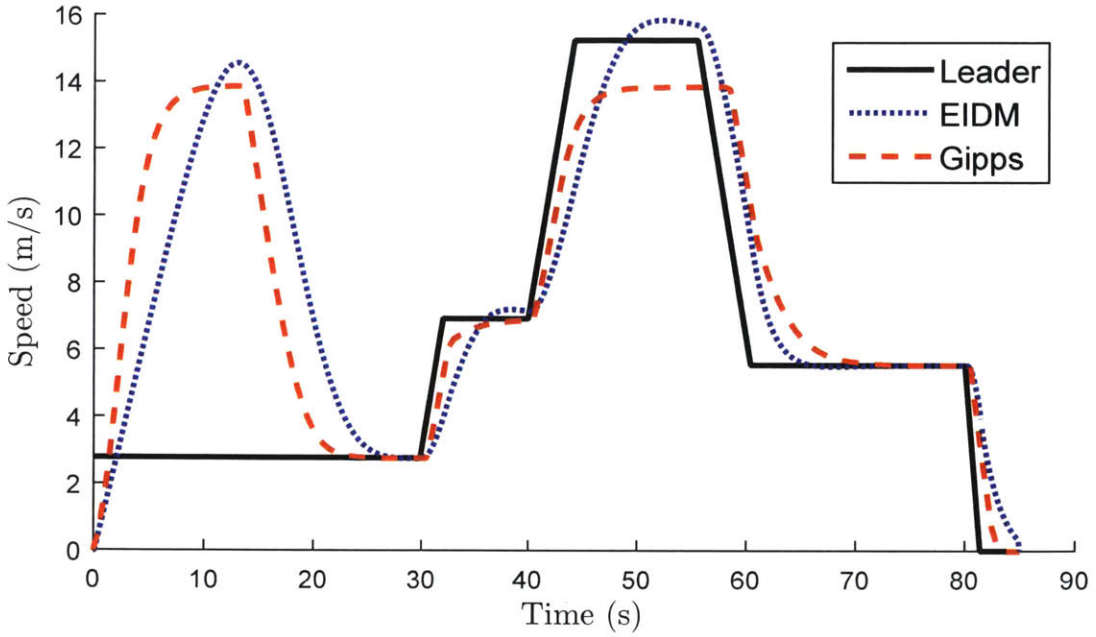

Figure 3.1: The response of an autonomous vehicle using EIDM and a manual vehicle using the Gipps car-following model to a leader.

vehicle penetration rate has on traffic dynamics in cities. This knowledge will help us to create an analytical model which incorporates the flow of autonomous vehicles in an urban network and can be used to find the optimal signal plans in mixed traffic scenarios.

The experiments involve a simple network which isolates a single signalized intersection. In the simulation environment, we created a single-lane road 300 meters long with a traffic light 120 meters from the entrance of the roadway, and a speed limit of 50 kilometers per hour. The traffic signal had a green phase between 10 and 60 seconds out of a 60 second cycle time. The remainder of the cycle time not allocated to the green phase is a red phase. When the green phase is 60 seconds long, the traffic light remains green at all times. Thus, the results at this green phase can be easily compared to a highway environment.

The autonomous vehicle penetration was varied between 0 and 100% in intervals of 10%. For each combination of penetration rate and green phase length, 30 simulation replications were run to gather a statistically valid sample, due to the stochastic nature of the traffic simulator we use. In each replication, the simulated throughput, measured by the number of vehicles which complete travel through the network, and the average travel time of vehicles in the network are recorded.

3.4 Results

In these experiments, we were mostly interested in investigating two aspects of the impact that automated driving may have on urban traffic. First, we analyzed the network capacity by analyzing how many vehicles were able to complete travel through the network per hour, given the limitations imposed by the traffic signal and resulting congestion. Experiments in highway scenarios have shown that increased autonomous vehicle penetration leads to increased network capacity, and so this will show whether these results can extend to urban settings as well.

We also examined the impact that autonomous vehicles have on average travel time within the network. Largely because of autonomous vehicles' reduced reaction time, introducing them into the urban network should allow traffic to disperse more quickly at a signalized intersection, leading to reduced travel time at the traffic signal. Examining how this travel time reduction varies may provide interesting insights into urban automated driving.

3.4.1 Network Capacity

To investigate network capacity, the demand rate was set to a very high rate, 5000 vehicles per hour, to observe the number of vehicles which could traverse the network in this scenario. Due to the structure of this simple network, with only a single source and a single sink and finite length, throughput increases monotonically as demand rate increases until reaching a maximum, which is the network capacity. Adding additional vehicles beyond 5000 per hour does not increase throughput, and so these experiments reveal how network capacity changes as the autonomous penetration rate changes.

Figures 3.2 and 3.3 show the impact on increased penetration rate of autonomous vehicles on the maximum throughput achieved by the network under various green phase lengths. Each curve shows a set of experiments run with the traffic signal set to a specific green phase length from 10 to 60 seconds, in increments of 5 seconds. In Figure 3.2, the autonomous vehicle penetration rate is on the x axis, while the y axis shows the maximum throughput achieved in terms of vehicles per hour. In Figure 3.3, the same curves are plotted with the y axis representing the percentage increase in maximum throughput from a baseline of 0% autonomous vehicle penetration.

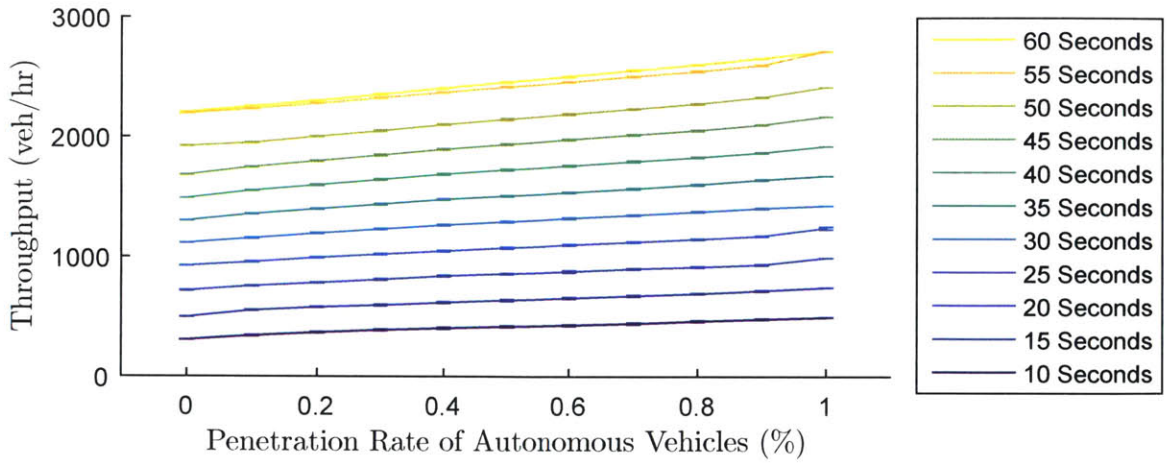

Figure 3.2: The maximum throughput achieved on a one-lane network with a single signalized intersection for different green phases and autonomous vehicle penetration rates.

From these curves, we can see that the maximum throughput achieved in the network increases monotonically as penetration rate of autonomous vehicles increases. This holds at all green phase lengths that were simulated. This means that as the penetration rate of autonomous vehicles flowing through an intersection increases, the maximum throughput of the intersection increases. Looking at the increase as a percentage, we can see in Figure 3.3 that the percentage increase is largest when the traffic signal has a short green phase. At 100% penetration rate of autonomous vehicles and a 10 second green phase, the maximum throughput achieved is a 60% increase over the maximum throughput achieved at 0% penetration rate. At larger green phases, the effect is less; there is a 27.8% increase with a 30

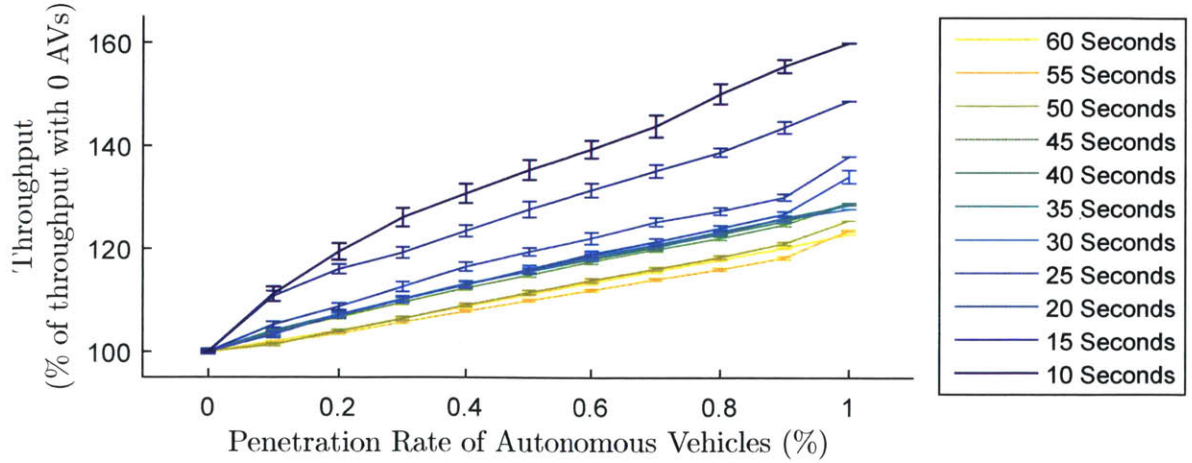

Figure 3.3: The maximum throughput achieved on a one-lane network with a single signalized intersection as a percentage of the baseline with no autonomous vehicles.

second green phase and a 22.9% increase with a 60 second green phase. The increase in intersection maximum throughput is much larger, as a percentage, with short green phases.

3.4.2 Travel Time Reduction

We also look at the impact that autonomous vehicle penetration has on the average travel time experienced by vehicles in the network. For these experiments, we used simulations featuring 15, 20, 25, and 30 second green phases. In each scenario, we varied the demand rate to cover cases with low traffic, moderate traffic, and heavy traffic, ranging between 300 and 1800 vehicles per hour. Figure 3.4 shows the results of these experiments displayed in four plots, each showing the results for a different green phase length. Each plot shows demand rate on the x axis and average travel time on the y axis. The curves represent the average travel time for autonomous vehicle penetration rates of 0%, 5%, 20%, 50%, and 100% as a function of the demand rate in the network.

Figure 3.4a displays the results of the experiments that consider a 15 second green phase. The demand rate in this plot varies between 300 and 1200 vehicles per hour, and each curve shows how average travel time varies as a result of changing demand rates for a particular level of autonomous vehicle penetration. The line represents the mean of 30 simulations, and the error bars show one standard deviation above and below the mean.

As demand rate increases, the average travel time also increases. At low demand rates, the traffic is in freeflow or near-freeflow conditions, with low travel times that do not increase with demand rate. In these conditions, more vehicles can be added to the network without causing additional travel time to the existing vehicles. At high demand rates, the traffic is nearly completely congested with high travel times that also do not change as demand rate is increased. At both of these extremes, there is little variance in the average travel time observed.

In between these two, moderate demand rates produce behavior much different than freeflow or fully congested conditions. Average travel time increases sharply with any increase in demand rate, and the variance is much higher than at low or high demand rates, indicating that individual simulations of the network produced widely varying results. By analyzing the differences between the curves representing different penetration rates, we observe that increasing the autonomous vehicle penetration rate appears to push the travel time curve to the right. Freeflow conditions are sustained at higher demand rates, and it requires a

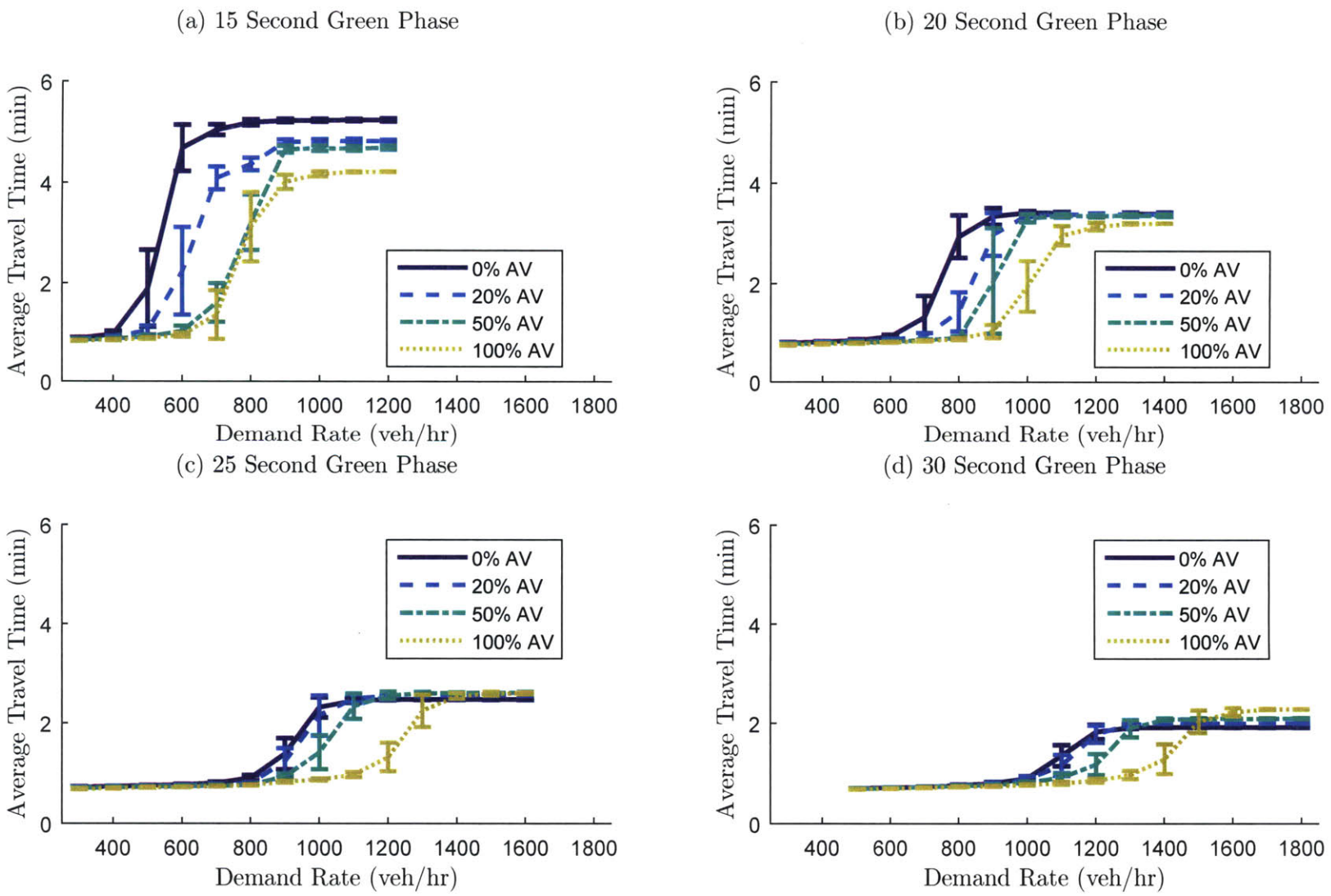

Figure 3.4: Average travel times obtained for different combinations of AV penetration rate, green phase, and demand rate via microscopic traffic simulation.

higher demand rate to fully congest the network. This leads to large differences in average travel time observed at moderate demand rates, where networks with low penetration rates of autonomous vehicles may approach congestion while networks with high penetration rates remain near freeflow. For example, with a 15 second green phase and a demand rate of 600 vehicles per hour, the average travel time with no autonomous vehicles is 4.68 minutes, while with 100% autonomous vehicles it is only 0.94 minutes, an 80% reduction in travel time. With only a 20% penetration rate, the average travel time is 2.24 minutes, a 53% reduction in travel time. In scenarios featuring longer green phases, the curves are shifted to the right and the maximum travel time is reduced due to the longer green phase. As green phase length increases, more vehicles are able to pass through the signalized intersection during each cycle. This means that congestion levels are reduced at all levels of demand rate.

At high demand rates and at longer green phases, such as in Figures 3.4c and 3.4d, it appears that increasing the penetration rate of autonomous vehicles actually increases the average travel time, that is that adding autonomous vehicles slows down the traffic. However, this result is likely due to the nature of the simulator and the finite length of the roads in the network. In the simulator, if a vehicle tries to enter a full roadway which does not have space for the entering vehicle, it waits outside the network in a virtual queue until space becomes available. Because of the faster reaction times of autonomous vehicles, the vehicles are more quickly able to create space in the network after the signal enters its green phase. With long green phases, this allows vehicles to enter the network from the virtual queue before the signal turns green again. Since travel time is recorded based on when the vehicle enters the physical network rather than the virtual queue, this results in an apparent higher travel time for high demand rates at long green phases. In larger networks where fewer vehicles are waiting in these virtual queues, this result is unlikely to hold.

These results illustrate the potential impact of switching vehicles on the network from manual to autonomous. This is potentially relevant as autonomous vehicles start seeing adoption and drivers replace their current manual vehicles with autonomous ones. It is of interest to understand how the traffic dynamics of cities will change in response to this switch. Using these curves, we can observe the change in travel time gained by switching some vehicles on the road to autonomous vehicles.

In this scenario, we can see that this switching will have the largest impact in roadways which feature moderate congestion due to demand rates in the middle of the range observed. At low demand rates, switching has little impact, and at high demand rates, the impact of

switching depends on the green phase lengths used. At a moderate demand rate, however, switching can potentially have enormous impacts, such as the 80% reduction in travel time observed before, or even a 53% reduction by switching one in five manually-driven cars to autonomous ones. It could thus be beneficial for cities to explore ways to focus the introduction of autonomous vehicles on roadways in this regime.

3.5 Conclusion

The simulation results presented in this chapter expand upon previous research in the field which focused on the traffic dynamics of mixed autonomous and non-autonomous traffic on highways. Using microscopic traffic simulation to model manually driven and autonomous vehicles with different car-following models and behavioral parameters, changes in traffic dynamics were observed in a small-scale urban environment featuring a signalized intersection. These results indicate that as autonomous vehicle penetration increases, network capacity increases and average travel time for vehicles in the network decreases. These positive impacts are similar to those found by existing literature on highway scenarios. In the next chapter, these results are used to develop an analytical model of traffic flow in an urban network featuring both manual and autonomous vehicles.

Chapter 4

Analytical Formulation

4.1 Introduction

The microscopic traffic simulation experiments in Chapter 3 provide a basis for the understanding of mixed autonomous and non-autonomous traffic in urban environments, which we can use to begin to understand the problem of traffic management in these environments. However, when analyzing the traffic dynamics of large-scale city networks, microscopic traffic simulation can quickly become computationally intensive due to the number of vehicles involved. In order to begin to approach large-scale urban transportation problems involving mixed traffic with both autonomous and manually driven vehicles, it will be helpful to develop analytical models of the network which accurately approximate the impacts observed via simulation.

This formulation provides a key step towards simulation-based optimization involving mixed autonomous and non-autonomous traffic in the future, where the queueing network model can be used to quickly approximate objective function values much more quickly than computationally intensive simulation runs. Similar queueing network models have been used in simulation-based optimization frameworks previously [33, 34]. Large-scale optimization problems, such as urban transportation problems, are often difficult to solve via simulation because they are prohibitively computationally intensive. These simulation-based optimization frameworks combine information obtained from a tractable analytical model with that obtained from the simulator in order to reduce the time needed to obtain solutions. In order to solve these transportation problems in scenarios involving fixed autonomous and non-autonomous traffic, a new analytical model formulation is needed due to the changes in traffic patterns we observe.

In this chapter, we extend a previously formulated analytical network queueing model to model mixed autonomous and non-autonomous traffic in an urban traffic network. First, the existing formulation for only non-autonomous traffic is discussed. Then, we present modifications to that formulation which model the impact of autonomous vehicles as observed

in the simulation results in Chapter 3. Finally, the extended analytical model is compared to simulation results in the simple network discussed previously, and in the large-scale urban network of Lausanne.

4.2 Queueing Network Model

We first define a system of equations for an analytical queueing network model, which we can use to find an analytical approximation of performance in a traffic network, before extending this model to apply to mixed traffic including autonomous vehicles. This queueing network model was proposed by Osorio and Bierlaire [35]. It differs from other traffic queueing models by approximating congestion via the use of blocking probabilities and interactions between queues within a network.

The network queueing model represents each lane of each road in the network as a queue, with intersections as servers which process vehicles from incoming queues. After completing service, a vehicle may enter a downstream queue so long as it is not blocked. The model uses the following notation, where the index i refers to a given queue:

γ_i:	external arrival rate to the queue;
λ_i:	total arrival rate to the queue;
μ_i:	service rate of the queue's server;
$\tilde{\mu}_i$:	unblocking rate of the server;
$\hat{\mu}_i$:	effective service rate (accounts for both service and eventual blocking);
P_i^f:	probability of being blocked at queue i;
p_{ij}:	transition probability from queue i to queue j;
k_i:	upper bound of the queue length;
N_i:	total number of vehicles in queue i
$P(N_i = k_i)$:	probability of queue i being full (blocking probability)
$\mathcal{I}^+$:	set of downstream queues of queue i.

The system of equations is given by:

$$\lambda_i = \gamma_i + \frac{\sum_j p_{ji}\lambda_j \left(1 - P\left(N_j = k_j\right)\right)}{\left(1 - P\left(N_i = k_i\right)\right)} \tag{4.1}$$

$$\frac{1}{\tilde{\mu}_i} = \sum_{j \in \mathcal{I}^+} \frac{\left(1 - P\left(N_j = k_j\right)\right)}{\left(1 - P\left(N_i = k_i\right)\right)\hat{\mu}_j} \tag{4.2}$$

$$\frac{1}{\hat{\mu}_i} = \frac{1}{\mu_i} + P_i^f \frac{1}{\tilde{\mu}_i} \tag{4.3}$$

$$P_i^f = \sum_j p_{ij} P(N_j = k_j) \tag{4.4}$$

$$P(N_i = k_i) = \frac{1 - \rho_i}{1 - \rho_i^{k_i+1}} \rho^{k_i} \tag{4.5}$$

$$\rho_i = \frac{\lambda_i}{\hat{\mu}_i} \tag{4.6}$$

For a full description of the queueing model formulation, refer to the original paper. All variables are endogenous, with the exception of γ_i, p_{ij}, and k_i, which are exogenous. These equations capture probabilities of blocking and spillbacks, which allow queues which become congested to create congestion in upstream queues.

Equations 4.1 through 4.4 define the between-queue interactions in the network. Equation 4.1 describes the total arrival rate in each queue as the sum of the external arrival rate into that queue from outside the network and the arrival rates from upstream queues. If the queue is full ($N_i = k_i$), the queue cannot receive vehicles from these other queues due to blocking. Equation 4.2 gives the unblocking rate $\tilde{\mu}_i$ at which spillbacks in queue i dissipate.

Equation 4.3 defines the effective service rate $\hat{\mu}_i$ at each queue, which accounts for service during states where the queue is not block and unblocking during states where it is. This expression is a function the exogenous variable μ_i, the service rate at a queue. The μ_i for each queue in the network are determined as a function of the saturation flow of that queue, which is the rate at which vehicles could leave the queue if it were unblocked and if any traffic signals were constantly in green phase. At a signalized intersection, this saturation flow is then multiplied by the sum of the green phase lengths corresponding to that queue divided by the total cycle time of the signal. Precisely, the μ_i for queues which are served by signalized intersections are determined by the following equation:

$$\mu_i = s \sum_{p \in \mathcal{P}_\mathcal{L}(i)} \frac{g_p}{c} \tag{4.7}$$

Here, s is the saturation flow, $\mathcal{P}_{\mathcal{L}}(i)$ is the set of intersection phases which permit movement of vehicles in queue i, g_p is the duration of one of these phases, and c is the total cycle time of the intersection.

Equation 4.4 defines the probability of service being blocked on a queue by multiplying the turning probabilities from the upstream queue to each downstream queue by the probability of that downstream queue being full.

Equations 4.5 and 4.6 give expressions for the blocking probabilities of each queue. Equation 4.5 defines the probability that a queue is full, using an expression derived from finite capacity queueing theory [36]. Equation 4.6 defines the traffic intensity of each queue as the ratio of the total arrival rate and the effective service rate.

4.3 Formulation with Mixed Autonomous Traffic

With the results obtained from our simulation of an isolated intersection, we can understand how the impact of autonomous vehicles in urban traffic and incorporate these impacts into our analytical network queueing model.

To enhance the existing network queueing model to more accurately reflect traffic dynamics in the presence of autonomous vehicles, we introduce a variable, α_i, which indicates the expected penetration rate of autonomous vehicles in queue i ($0 \leq \alpha_i \leq 1, \forall i$). This is an exogenous parameter, which requires some assumptions. First, we assume that the distribution of autonomous vehicle penetration on each queue within the network is known beforehand. In the simulation environment, this is easy to achieve. In practice, this may be estimated using sensors or other detection technologies. Second, we assume that the vector α of all penetration rates does not change as other parameters change, including the green phases selected for the intersections.

Because we observed from the simulation results that the maximum throughput of an intersection increases as the α_i of the incoming lanes increases, we choose to alter the previously described queueing model by modeling the service rates of each queue as a function of the penetration rate of autonomous vehicles in that queue. Previously, the service rates of the queues were given by the capacity of the underlying lanes. For signalized intersections, the capacity of a lane is the product of its saturation flow and the proportion of green time allocated to that lane per cycle, as provided in Equation 4.7. Based on our results, which

show that the saturation flow of a lane increases roughly linearly as the penetration rate of autonomous vehicles on that lane increases, we formulate the following expression for the effective saturation flow of each queue:

$$s_i^{\text{eff}} = s_1 \alpha_i + s_0 (1 - \alpha_i) \tag{4.8}$$

Here, s_0 is the variable previously defined as s, the saturation flow with 0% autonomous vehicles, and s_1 is the saturation flow with 100% autonomous vehicles. Equation 4.8 provides s_i^{eff}, the effective saturation flow of queue i as a function of α_i, the penetration rate of autonomous vehicles on that queue. This value is a linear interpolation of the saturation flow with no autonomous vehicles and the saturation flow with only autonomous vehicles. Through our simulation results, we estimated s_0 to be 2100 vehicles per hour and s_1 to be 2800 vehicles per hour, so these values were used in the new formulation.

By taking Equation 4.7 and replacing the saturation flow s with this new penetration rate dependent effective saturation flow s_i^{eff}, the service rate of each queue is adjusted by the penetration rate of autonomous vehicles on each queue as follows:

$$\mu_i = s_i^{\text{eff}} \sum_{p \in \mathcal{P}_{\mathcal{L}}(i)} \frac{g_p}{c} \tag{4.9}$$

These updated μ_i are used in the queueing network model described in equations 4.1 through 4.6 to formulate the model with mixed autonomous and non-autonomous traffic.

4.4 Network Model Evaluation

To evaluate how closely this extended analytical network queueing model approximates trends observed in simulation, we compare the average travel times estimated by solving this analytical model to the average travel times observed via microscopic traffic simulation. We first compare these results in the single-lane network with a single traffic signal which was used in Chapter 3. Then, we use the Lausanne city network model to compare the performance in a large-scale urban network.

We compared the average travel time obtained in microscopic traffic simulation over the simple network described previously with the estimate of expected travel time obtained via

the analytical network queueing model. The average travel time for the simulated network was obtained as described previously. The expected travel time estimated by the analytical queueing model was obtained using Little's law [37], $L = \lambda W$, where L is the expected number of vehicles in the system, λ is the arrival rate of vehicles into the system, and W is the expected time that vehicles spend in the system. Little's law shows that the expected time that vehicles spend in the system is the ratio of the expected number of vehicles in the system to the arrival rate of vehicles into the system. The expected time that vehicles spend in the system, an approximate of the travel time, can therefore be found by this equation provided by Osorio and Chong [33]:

$$\frac{\sum_i E[N_i]}{\sum_i \gamma_i (1 - P(N_i = k_i))} \tag{4.10}$$

The numerator of Equation 4.10 sums the expected number of vehicles present in each queue i, while the denominator represents the effective arrival rate into the network. To find $E[N_i]$, the expected number of vehicles in queue i, we use the following equation derived by Osorio and Chong [33]:

$$E[N_i] = \rho_i \left(\frac{1}{1 - \rho_i} - \frac{(k_i + 1)\rho_i^{k_i}}{1 - \rho_i^{k_i+1}} \right) \tag{4.11}$$

4.4.1 Single-Lane Network

Using the network described in Chapter 3 and the supply and demand scenarios analyzed in Section 3.4.2, the queueing network model was used to find the expected travel time. For each combination of demand rate, autonomous vehicle penetration rate, and green phase length, Equations 4.1 through 4.6 were solved with service rates defined as described by Equation 4.9. Then, expected travel time was found by evaluating Equation 4.10. The results are presented in Figure 4.1 and compared to the analogous simulation results previously presented. The simulation plots, Figures 4.1a, 4.1c, 4.1e, and 4.1g, are the same as shown in Figure 3.4. Figures 4.1b, 4.1d, 4.1f and 4.1h show the expected travel times estimated by the analytical queueing network model:

Each point on the plots showing results of the network queueing model show expected travel time of vehicles in the network for a given demand rate, autonomous vehicle penetration rate, and green phase. Each point on the plots showing simulation results represents the

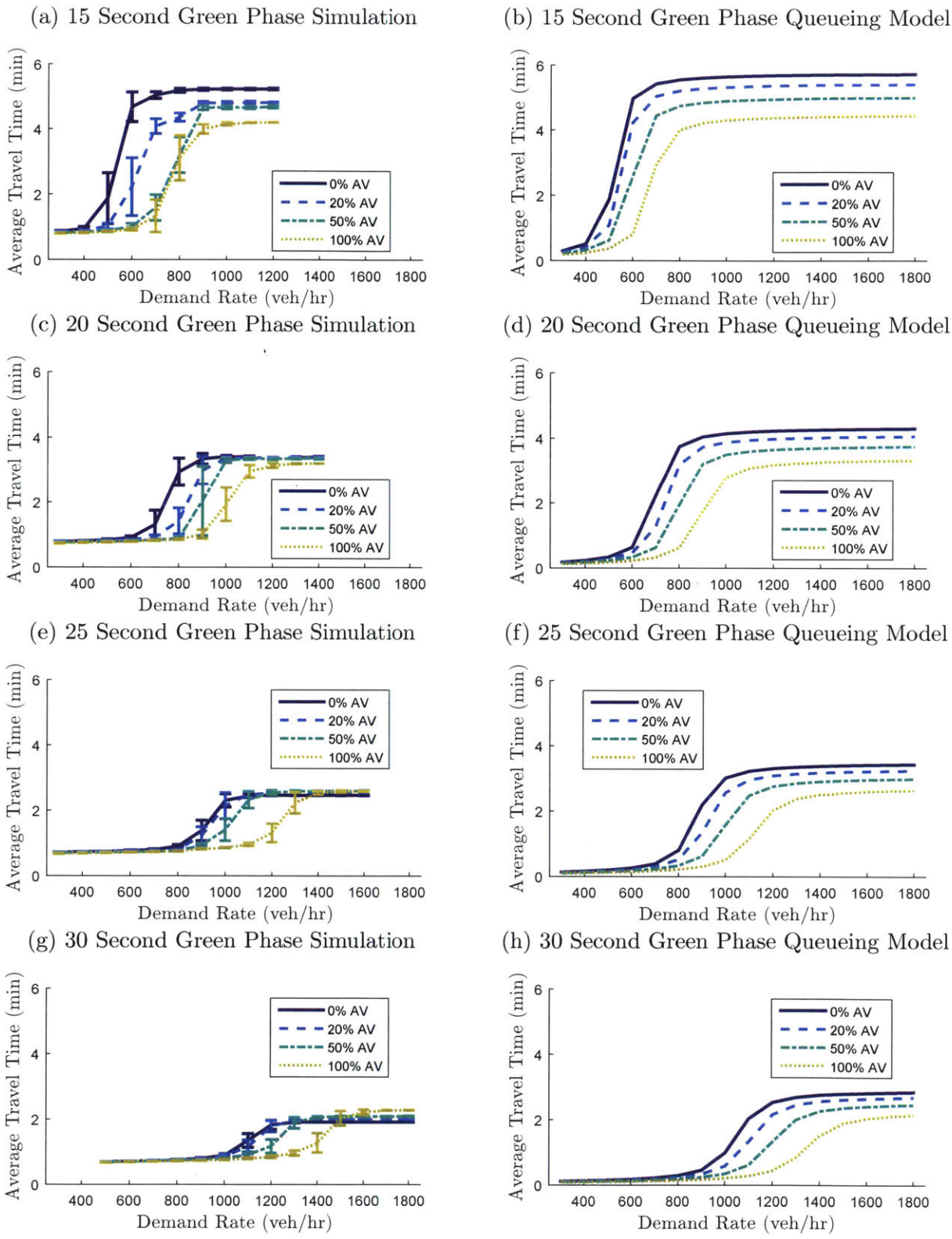

Figure 4.1: Average travel times obtained for different combinations of AV penetration rate, green phase, and demand rate via microscopic traffic simulation (a, c, e, g) and via solving the updated queueing network model (b, d, f, h).

observed average travel time of vehicles in the network for the same scenario, with error bars showing plus or minus one standard deviation from the mean, obtained via 30 simulation replications. Each curve displays the results for a particular penetration rate of autonomous vehicles in the network (0%, 20%, 50%, or 100%), and each subplot represents a different green phase used for the signalized intersection in the network.

By comparing the simulation results to those provided by evaluation of the queueing model for the same green phase length, we can observe how closely the analytical model approximates simulation results. By and large, we observe the same trends described in Section 3.4.2 in the results of the queueing model. At low demand rates, expected travel times are low and do not vary as autonomous vehicle penetration changes. At moderate demand rates, there are large differences in expected travel times for different penetration rates, where large penetration rates are able to achieve significant savings in travel time. At high demand rates, the results are somewhat different between the simulation and analytical model results, as the analytical model results show small reductions in travel time as autonomous vehicle penetration rate increases while the simulated results show savings only with a 15 second green phase length, and minor travel time increases at higher green phase lengths. However, as described previously, these increases can be attributed to virtual queues in the simulator, so this inconsistency between the simulator and the queueing model does not warrant concern. In addition to the general trends captured by the queueing model, the magnitude of travel times are also similar between the two sets of results, especially at moderate and high demand rates. At low demand rates, much of the travel time in the simulator consists of the time a vehicle spends traversing the length of the road, with no delay component. Because the queueing model does not incorporate free flow travel time into its estimate of travel time, this disparity is unsurprising.

These figures show that the updated queueing model is able to capture a great deal of the characteristics of travel time as they vary with autonomous vehicle penetration, green phase length, and demand rate. For both the simulation results and the analytical results from the updated queueing model, we observe the same S-shaped curve present at any given level of penetration rate and green phase. Additionally, we see that curves with increasing penetration rate generally fall below those curves with higher penetration rate, indicating travel time savings as more autonomous vehicles are added to the network. This holds true for both the simulation results and the queueing model solutions.

4.4.2 Lausanne City Network

Additionally, we compare the performance of the analytical queueing model compared to simulation in a network based on an existing city network in Lausanne, Switzerland. This network was used in previous research with the existing queueing model [33,38], and relatively accurate estimates of simulated travel times were obtained. The network contains 603 roads and 231 intersections, and the queueing model representation consists of 902 queues. For more details regarding the network, refer to Dumont and Bert [39].

We determined a highly varying spatial distribution of autonomous vehicles by allocating autonomous vehicles only to the origins and destinations which experience the most travel time savings from increased autonomous vehicle penetration. To select these origins and destinations, the network was simulated 50 times with all origin-destination pairs having equal penetration rate of autonomous vehicles, with penetration rates ranging from 0% to 100% in increments of 5%. By finding the number of vehicles that travel between each origin and destination and the average duration of those trips at each level of penetration, we were able to find the largest travel time savings across origins and destinations using the following formulas:

$$S_i = -\sum_{j\in\mathcal{D}}\sum_{\alpha}\frac{n_{ij\alpha}\left(t_{ij\alpha}-t_{ij0}\right)}{\sum_i\sum_j n_{ij\alpha}} \quad \forall i \in \mathcal{O} \tag{4.12}$$

$$S_j = -\sum_{i\in\mathcal{O}}\sum_{\alpha}\frac{n_{ij\alpha}\left(t_{ij\alpha}-t_{ij0}\right)}{\sum_i\sum_j n_{ij\alpha}} \quad \forall j \in \mathcal{D} \tag{4.13}$$

Equation 4.12 describes S_i, the total percentage savings of travel time for traffic originating from origin i. $n_{ij\alpha}$ is the average number of vehicles which travel from origin i to destination j with an autonomous penetration rate α, as observed in the simulations. $t_{ij\alpha}$ is the average travel time for vehicles that complete travel between origin i and destination j at penetration rate α, and t_{ij0} is this travel time in the case where $\alpha = 0$ and no autonomous vehicles are present. S_i is the sum for a given origin, across all destinations in the set of destinations $\mathcal{D}$ and all penetration rates simulated, of the product of the proportion of all vehicles in the network which traveled from origin i to destination j and the reduction in average travel time compared to the baseline travel time with no autonomous vehicles in the network. Equation 4.13 describes S_j, which is a similar sum, but for a given destination and across all origins in the set of origins $\mathcal{O}$.

The quantities S_i and S_j are used as scores to evaluate which origins and destinations experience the largest reduction in travel times as autonomous vehicles are added to the network. If the average travel time for trips involving a given origin decreases as penetration rate increases, its score will be higher. This score increase will be highest for those origins and destinations which feature a large number of trips relative to the number of vehicles traveling in the network. After finding these scores for each origin and destination using the results of the simulation runs, all origins with $S_i > 50$ and all destinations with $S_j > 50$ were chosen to feature autonomous vehicles. Five origins and eight destinations were chosen this way. Autonomous vehicles were allocated to all origin-destination pairs involving one of these five origins and/or one of these eight destinations, resulting in a total of 619 origin-destination pairs which included autonomous vehicles.

Once these origins and destinations were chosen, the origin-destination matrix at a given penetration rate α_{global} was created by setting the fraction of autonomous vehicles for all trips originating at one of the chosen origins and/or terminating at one of the given destinations equal to α_{global}, while for all other origin-destination pairs the fraction of autonomous vehicles was zero. This creates a highly non-uniform distribution of autonomous vehicles across the links of the network, and also means that the true global penetration rate of autonomous vehicles on the network is less than α_{global}. When $\alpha_{\text{global}} = 1$, 44% of trips are taken by autonomous vehicles. This uneven distribution makes the understanding of the impact of autonomous vehicles more important, as the saturation flows of each link will vary depending on the penetration rate on that link. Once the origin-destination matrix was established, 50 simulation replications were run with α_{global} at every increment of 0.05 between 0 and 1 to estimate the α_i on each lane of the network, which were used to create the extended queueing network model.

Figures 4.2 and 4.3 show how the analytical model compares to the simulation results for the Lausanne city network with autonomous vehicles allocated as described above. On the x-axis is the global penetration rate, meaning the percentage of trips at the selected origin-destination pairs which are autonomous vehicles. The y-axis in Figure 4.2 displays the average travel time in minutes, while in Figure 4.3 the y-axis represents the average travel time at each penetration rate as a percentage of the average travel time with no autonomous vehicles. The two curves display the results from simulation in blue and from the queueing model in red. The simulation results include error bars displaying two standard deviations above and below the mean.

Once again, the analytical queueing model is able to capture the trends of average

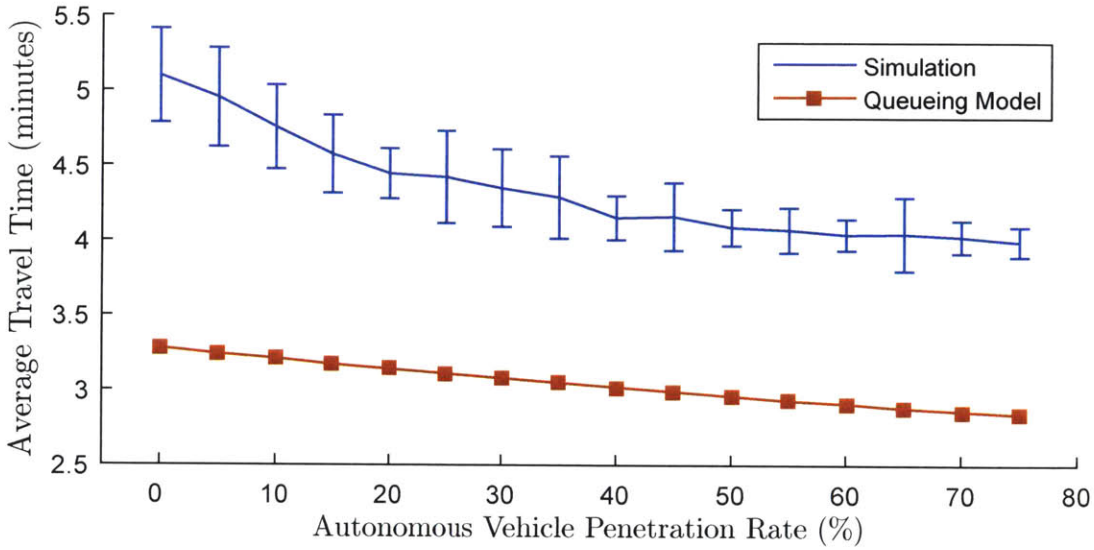

Figure 4.2: The average travel times in the Lausanne city network found by microscopic traffic simulation (with error bars) and the expected travel times found by solving the analytical queueing model (squares) at various levels of autonomous vehicle penetration.

travel time as penetration rate changes. For both the simulation results and the analytical results, the average travel time is nearly monotonically decreasing as the penetration rate of autonomous vehicles increases. However, the queueing model significantly and systematically underestimates the value of the travel times, by roughly 1.5 to 2 minutes. Meanwhile, Figure 4.3 shows that the queueing model underestimates the relative reduction in average travel times relative to the baseline of no autonomous vehicles. Although the direction of the trends are the same, the simulation results display significantly larger travel time savings as autonomous vehicle penetration increases.

These inaccuracies are somewhat expected due to the large, complex nature of the Lausanne city network. With the large number of queues in the network, network effects may be present that are difficult to model with an analytical queueing formulation. However, capturing network-wide trends with a formulation which is based on the results of a single-intersection simulation experiment is a promising result that indicates that autonomous vehicles' impacts on traffic dynamics may be approximated by analytical methods rather than simulation.

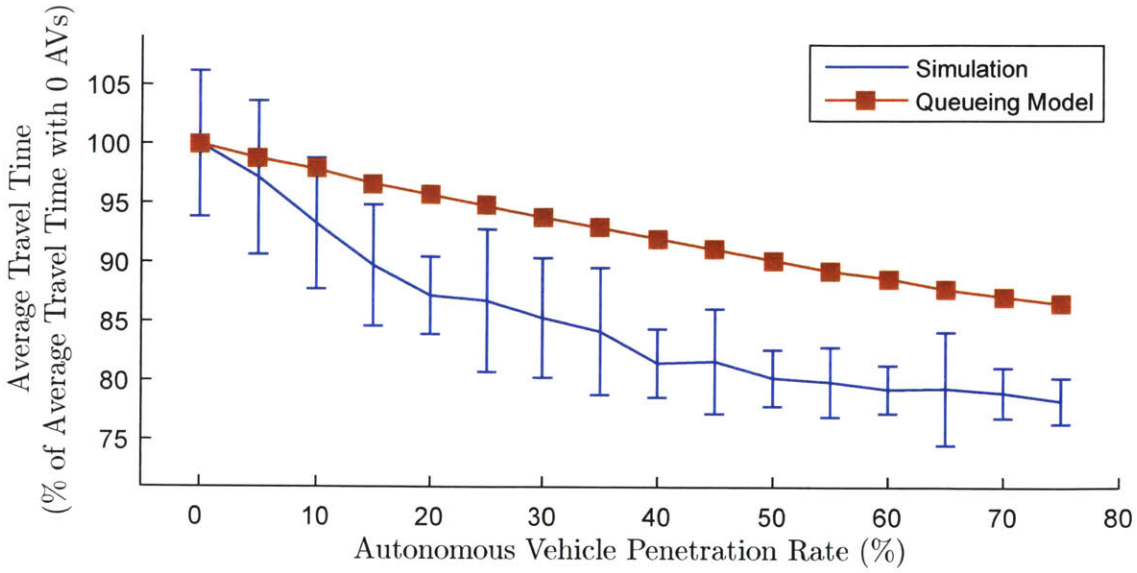

Figure 4.3: The same travel times as in Figure 4.2 plotted as a percentage of the baseline with no autonomous vehicles.

4.5 Conclusion

By extending an analytical network queueing model to incorporate the impacts of autonomous vehicles in urban traffic, we formulate a tractable and scalable model which accurately approximates the behavior of mixed autonomous and non-autonomous traffic in urban environments. This model is an extension of an existing formulation of an analytical queueing network model for urban traffic which incorporates the impact of autonomous vehicles by adjusting the service rates of the queues. An increase in autonomous vehicle penetration rate results in an increased service rate, consistent with the simulation results presented in Chapter 3.

As opposed to microscopic simulation models, which are detailed yet computationally intensive, the analytical model detailed in this chapter provides an opportunity to quickly obtain approximations of traffic behavior in large-scale urban networks. In the future, this capability could be used to support research to solve large-scale transportation planning and traffic management problems. Specifically, this analytical model can be incorporated into an existing framework for simulation-based optimization which combines information from a simulator with estimates obtained by solving the analytical queueing model. In this way, this research provides an initial step towards an optimization framework which can be used to determine how traffic management strategies should respond to the introduction of autonomous vehicles into urban traffic.

Chapter 5

Conclusion

5.1 Discussion

We present the results of several simulation experiments which provide insight into the impacts that the introduction of automated or semi-automated vehicles may have on traffic networks. The existing research in this area has mostly focused on the simulation of these vehicles have in highway scenarios. We extend the existing research on this subject by simulating mixed autonomous and human traffic in urban scenarios to establish an understanding of the impacts specific to cities, and formulating a novel analytical network queueing model which can be used to quickly evaluate metrics of traffic performance in large-scale urban networks. These approaches provide preliminary understanding of how traffic patterns change due to increased autonomous vehicle penetration and initial steps towards the development of new traffic management strategies which respond to these changes.

In Chapter 2, we review the literature on behavioral models which have been used to represent autonomous vehicles in microscopic traffic simulation. Lots of literature featured simulations of highway scenarios using adaptive cruise control and cooperative adaptive cruise control models to represent autonomous vehicles in mixed autonomous and non-autonomous traffic. These simulation experiments largely indicate positive impacts as the autonomous vehicle penetration rate increases. These positive impacts include increased capacity, increased traffic stability, and faster recovery from traffic breakdowns.

In Chapter 3, we select different behavioral models to represent semi-automated and human-driven vehicles in urban traffic. The Enhanced Intelligent Driver Model (EIDM) was selected for autonomous vehicles based on its ability to provide realistic results at all speeds and its adoption in test semi-automated vehicles in the real world. The Gipps model was selected for manual vehicles based on field studies which demonstrate a good approximation of actual traffic flow.

We used microscopic traffic simulation to observe how this mixed traffic behaves on a

single-lane network with a signalized intersection at varying green phases, demand rates, and autonomous vehicle penetration rates. The results indicate that increasing autonomous penetration has similar impacts in urban scenarios as the existing literature indicates it does in highway scenarios. As the AV penetration rate was increased on this simple network, the capacity of the roadway increased as well, meaning that more vehicles could pass through the intersection during the same duration of green phase. Additionally, the average travel time experienced by vehicles in the network was reduced as autonomous penetration increased. In conditions of moderate congestion, this reduction was significant.

These findings are generally in agreement with the literature on the simulation of ACC and CACC equipped vehicles on highways, which find that autonomous and semi-autonomous vehicles have the potential to increase capacity and average speed in these scenarios. Our research shows promise that these benefits will not be limited to highways, but will apply to urban roads as well. However, the specific selection of behavioral models used may have a large impact on the specific impacts observed. Choosing different behavioral models and parameters may yield different impacts on traffic flow.

In Chapter 4, we present an analytical queueing network model which extends an existing model to approximate the effects of autonomous vehicles. The existing model incorporates the impacts of spillbacks and blocking on upstream and downstream queues within the network. Based on the simulation results presented in Chapter 3, we introduce an exogenous variable representing the autonomous vehicle penetration on each queue in the network and redefine the service rates of queues in the network to increase as this autonomous vehicle penetration rate increase. Using Little's law, we evaluate the expected travel time experienced by vehicles in two networks and compare them to simulation results. Results on the single-lane network defined in Chapter 3 show similar patterns of travel time resulting from different combinations of autonomous vehicle penetration rate, demand rate, and green phase length. Results on the large-scale Lausanne city network show similar decreasing trends in travel time as autonomous vehicle penetration rate increases, which are captured in both simulation and the analytical formulation.

5.2 Future Work

This research, which extends autonomous vehicle simulation research to the field of urban traffic, presents many opportunities for further investigation. The chief result of this research which will be expanded upon in the future is the formulation of an analytical queueing

network model which approximates the behavior of mixed autonomous and human-driven traffic in large-scale urban scenarios. This model presents an opportunity in the future for large-scale optimization of transportation problems in the context of mixed autonomous traffic. This model can be incorporated into existing simulation-based optimization frameworks which combine information from the analytical model and a simulator to efficiently solve these optimization problems. In this way, this research works towards the larger goal of understanding how traffic management strategies in urban environments may change as autonomous vehicles are introduced into city transportation systems.

In addition to this possibility, the research presented in this thesis contains other open-ended questions which can be explored to help expand upon the topics it discusses. While this thesis focuses on the simulation of signalized intersections and an analytical queueing model based on the impact that autonomous vehicles have on traffic in that context, there are many more contexts in which the impact of autonomous vehicles remains unexplored. Investigating these possibilities would be able to provide more answers to the questions of how urban traffic will respond to an increase in automated driving.

Additionally, it is easy to envision different realities for autonomous vehicles than the ones which we assumed for most of this research. One intriguing possibility is the potential for autonomous vehicles to serve as a driverless taxi system. In this case, the introduction of autonomous vehicles would not simply replace human drivers one-to-one, but instead one autonomous vehicle could handle several human trips. Another way that autonomous vehicles could differ from the ones envisioned in this research is by featuring higher levels of automation, potentially including lane changing functionality. Simulation of highly or fully automated vehicles could reveal additional impacts on traffic behavior and unlock additional options in traffic management.

All of these potential avenues of research show that there remains much more unknown about the impacts of automated driving than known. In order to provide cities with the best opportunities to appropriately respond to the changes in transportation networks caused by autonomous vehicles, it is crucial that researchers continue to explore the widespread implications that automated driving will have on transportation systems. In this way, cities can be prepared to adapt quickly to a rapidly changing landscape of urban mobility.

Bibliography

[1] Google self-driving car project. Google. Accessed: August 11, 2016. [Online]. Available: https://www.google.com/selfdrivingcar/faq/

[2] (2016, May) Steel city's new wheels. Uber. Accessed: August 11, 2016. [Online]. Available: https://newsroom.uber.com/us-pennsylvania/new-wheels/

[3] A. Sage. (2016, January) Tesla curbs autopilot feature, but Musk says better than human driver. Reuters. Accessed: August 11, 2016. [Online]. Available: http://www.reuters.com/article/us-tesla-autopilot-idUSKCN0UO0NM20160110

[4] N. DuPuls, C. Martin, and B. Rainwater, "City of the future: Technology and mobility," Center for City Solutions and Applied Research, National League of Cities, Tech. Rep., 2015. [Online]. Available: http://www.nlc.org/find-city-solutions/city-solutions-and-applied-research/city-of-the-future

[5] "Preliminary statement of policy concerning automated vehicles," National Highway Traffic Safety Administration, Tech. Rep., 2013. [Online]. Available: http://www.nhtsa.gov/staticfiles/rulemaking/pdf/Automated_Vehicles_Policy.pdf

[6] S. Singh, "Critical reasons for crashes investigated in the national motor vehicle crash causation survey," National Highway Traffic Safety Administration, Tech. Rep., 2015. [Online]. Available: https://crashstats.nhtsa.dot.gov/Api/Public/ViewPublication/812115

[7] A. Kesting, M. Treiber, M. Schönhof, and D. Helbing, "Adaptive cruise control design for active congestion avoidance," *Transportation Research Part C: Emerging Technologies*, vol. 16, no. 6, pp. 668–683, 2008.

[8] N. Bailey, C. Osorio, A. Antunes, and L. Vasconcelos, "Designing traffic management strategies for mixed urban traffic environments with both autonomous and non-autonomous vehicular traffic," in *Mobil.TUM International Scientific Conference on Mobility and Transport*, Munich, Germany, 2015.

[9] A. Kesting, M. Treiber, and D. Helbing, "Enhanced intelligent driver model to access the impact of driving strategies on traffic capacity," *Philosophical Transactions of the Royal Society of London A: Mathematical, Physical and Engineering Sciences*, vol. 368, no. 1928, pp. 4585–4605, 2010.

[10] S. E. Shladover, D. Su, and X.-Y. Lu, "Impacts of cooperative adaptive cruise control on freeway traffic flow," *Transportation Research Record: Journal of the Transportation Research Board*, vol. 2324, no. 1, pp. 63–70, 2012.

[11] I. A. Ntousakis, I. K. Nikolos, and M. Papageorgiou, "On microscopic modelling of adaptive cruise control systems," *Transportation Research Procedia*, vol. 6, pp. 111–127, 2015.

[12] M. Segata, F. Dressler, R. Lo Cigno, and M. Gerla, "A simulation tool for automated platooning in mixed highway scenarios," in *Proceedings of the 18th Annual International Conference on Mobile Computing and Networking*. Association for Computing Machinery, 2012, pp. 389–392.

[13] M. Treiber, A. Hennecke, and D. Helbing, "Congested traffic states in empirical observations and microscopic simulations," *Physical Review E*, vol. 62, no. 2, p. 1805, 2000.

[14] A. Kesting, M. Treiber, M. Schönhof, F. Kranke, and D. Helbing, "Jam-avoiding adaptive cruise control (ACC) and its impact on traffic dynamics," in *Traffic and Granular Flow '05*. Springer, 2007, pp. 633–643.

[15] J. Wang and R. Rajamani, "Adaptive cruise control system design and its impact on highway traffic flow," in *Proceedings of the 2002 American Control Conference*, vol. 5. IEEE, 2002, pp. 3690–3695.

[16] S. E. Shladover, C. Nowakowski, J. O'Connell, and D. Cody, "Cooperative adaptive cruise control: Driver selection of car-following gaps," in *17th ITS World Congress*, 2010.

[17] G. M. Arnaout and J.-P. Arnaout, "Exploring the effects of cooperative adaptive cruise control on highway traffic flow using microscopic traffic simulation," *Transportation Planning and Technology*, vol. 37, no. 2, pp. 186–199, 2014.

[18] B. Van Arem, C. J. Van Driel, and R. Visser, "The impact of cooperative adaptive cruise control on traffic-flow characteristics," *IEEE Transactions on Intelligent Transportation Systems*, vol. 7, no. 4, pp. 429–436, 2006.

[19] K. Jerath and S. N. Brennan, "Analytical prediction of self-organized traffic jams as a function of increasing ACC penetration," *IEEE Transactions on Intelligent Transportation Systems*, vol. 13, no. 4, pp. 1782–1791, 2012.

[20] D. C. Gazis, R. Herman, and R. B. Potts, "Car-following theory of steady-state traffic flow," *Operations Research*, vol. 7, no. 4, pp. 499–505, 1959.

[21] R. Sukthankar, J. Hancock, S. Baluja, D. Pomerleau, and C. Thorpe, "Adaptive intelligent vehicle modules for tactical driving," in *1996 AAAI Workshop on Intelligent Adaptive Agents*, 1996, pp. 13–22.

[22] J. Hunt and G. Lyons, "Modelling dual carriageway lane changing using neural networks," *Transportation Research Part C: Emerging Technologies*, vol. 2, no. 4, pp. 231–245, 1994.

[23] J. Forbes, T. Huang, K. Kanazawa, and S. Russell, "The BATmobile: Towards a Bayesian automated taxi," in *International Joint Conference on Artificial Intelligence*, vol. 95, 1995, pp. 1878–1885.

[24] J. H. Yoo and R. Langari, "Stackelberg game based model of highway driving," in *ASME 2012 5th Annual Dynamic Systems and Control Conference joint with the JSME 2012 11th Motion and Vibration Conference*. American Society of Mechanical Engineers, 2012, pp. 499–508.

[25] A. Bose and P. Ioannou, "Mixed manual/semi-automated traffic: a macroscopic analysis," *Transportation Research Part C: Emerging Technologies*, vol. 11, no. 6, pp. 439–462, 2003.

[26] M. W. Levin and S. D. Boyles, "A multiclass cell transmission model for shared human and autonomous vehicle roads," *Transportation Research Part C: Emerging Technologies*, vol. 62, pp. 103–116, 2016.

[27] TSS-Transport Simulation Systems, "AIMSUN," Barcelona, Spain, 2015. [Online]. Available: https://www.aimsun.com

[28] D. Manstetten, W. Krautter, and T. Schwab, "Traffic simulation supporting urban control system development," in *4th World Congress on Intelligent Transportation Systems*, Berlin, Germany, 1997, pp. 1–8.

[29] S. Panwai and H. Dia, "Comparative evaluation of microscopic car-following behavior," *IEEE Transactions on Intelligent Transportation Systems*, vol. 6, no. 3, pp. 314–325, 2005.

[30] J. Barceló and J. Casas, "Dynamic network simulation with AIMSUN," in *Simulation Approaches in Transportation Analysis*. Springer, 2005, pp. 57–98.

[31] P. G. Gipps, "A behavioural car-following model for computer simulation," *Transportation Research Part B: Methodological*, vol. 15, no. 2, pp. 105–111, 1981.

[32] D. Levinson, A. Boies, J. Cao, and Y. Fan, "The transportation futures project: Planning for technology change," Minnesota Department of Transportation, Tech. Rep., 2016. [Online]. Available: http://conservancy.umn.edu/bitstream/handle/11299/177640/MnDOT2016-02.pdf

[33] C. Osorio and L. Chong, "A computationally efficient simulation-based optimization algorithm for large-scale urban transportation problems," *Transportation Science*, vol. 49, no. 3, pp. 623–636, 2015.

[34] C. Osorio and M. Bierlaire, "A simulation-based optimization approach to perform urban traffic control," in *TRISTAN VII, Triennial Symposium on Transportation Analysis*, Tromsø, Norway, 2010.

[35] C. Osorio, "Mitigating network congestion: analytical models, optimization methods and their applications," Ph.D. dissertation, École Polytechnique Fédérale de Lausanne, 2010. [Online]. Available: https://infoscience.epfl.ch/record/142940/files/EPFL_TH4615.pdf

[36] P. P. Bocharov, C. D'Apice, and A. Pechinkin, *Queueing theory*. Walter de Gruyter, 2003.

[37] J. D. Little and S. C. Graves, "Little's law," in *Building Intuition*. Springer, 2008, pp. 81–100.

[38] C. Osorio and M. Bierlaire, "A surrogate model for traffic optimization of congested networks: an analytic queueing network approach," *Report TRANSP-OR*, vol. 90825, pp. 1–23, 2009.

[39] A. Dumont and E. Bert, "Simulation de l'agglomération lausannoise simlo," Laboratoire des voies de circulation, ENAC, École Polytechnique Fédérale de Lausanne, Lausanne, Switzerland, Tech. Rep., 2006.